ADVANCED FUNCTIONAL MATERIALS

Supporting Information

for *Adv. Funct. Mater.,* DOI: 10.1002/adfm.202200830

Sharing of Strain Between Nanofiber Forests and Liquid Crystals Leads to Programmable Responses to Electric Fields

Sangchul Roh, John Kim, Divya Varadharajan, Joerg Lahann, and Nicholas L. Abbott**

Supporting Information

Sharing of Strain Between Nanofiber Forests and Liquid Crystals Leads to Programmable Responses to Electric Fields

Sangchul Roh, John Kim, Divya Varadharajan, Joerg Lahann and Nicholas L. Abbott**

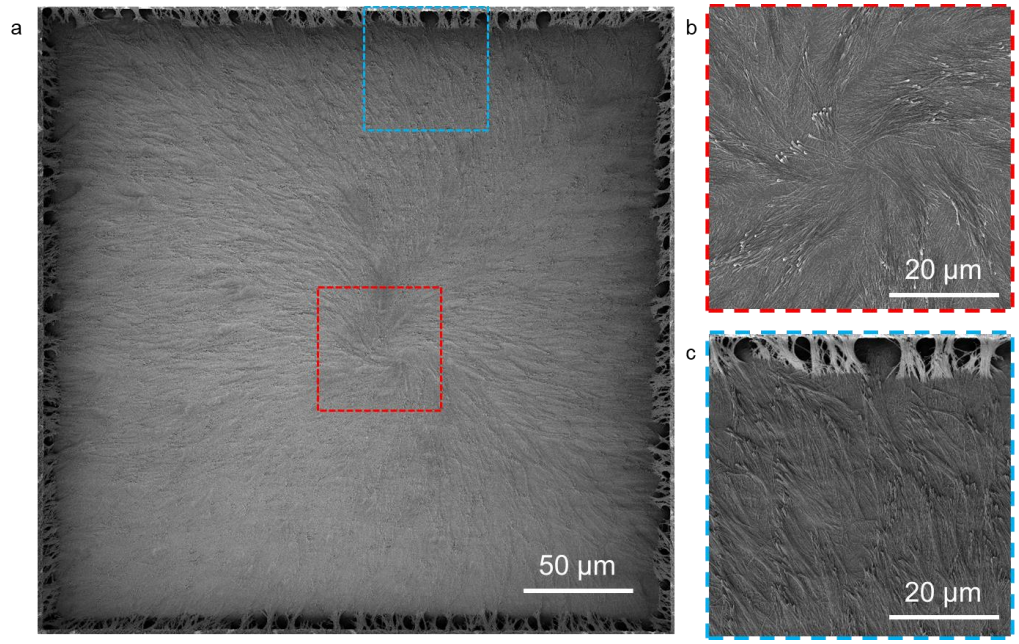

Figure S1. SEM images of NFF in Figure 1h-j at a) low magnification and b,c) high magnification. The area in (b,c) was selected from the boxed locations in a. The brightness of b) was adjusted using ImageJ.

The retardance of an LC film is given by,

$$\Delta r = \int_0^d \left(\frac{n_e n_o}{\sqrt{n_o^2 \sin^2\theta + n_e^2 \cos^2\theta}} - n_o \right) dz \quad \text{(S1)}$$

where n_e and n_o are the extraordinary refractive index (≈ 1.6) and the ordinary refractive index (≈ 1.48) of PCH, respectively.

With weak anchoring, the tilt angle of LC at air and a solid substrate is given by[1]

$$\theta_d = \bar{\theta}_d + \frac{L_d}{d + L_0 + L_d}(\bar{\theta}_0 - \bar{\theta}_d) \qquad (S2)$$

where $\bar{\theta}_0$ and $\bar{\theta}_d$ are the tilt angle of the easy axis at z=0 and d. L_0 and L_d are extrapolation lengths (K/W) at z = 0 and d. K and W are the Frank-Oseen elastic constant and anchoring energy of PCH. By reorganizing S2, we obtain

$$\frac{\bar{\theta}_d - \theta_d}{\bar{\theta}_d - \bar{\theta}_0} = \frac{L_d}{\left(\frac{K}{w_0}\right) + d + L_d} \qquad (S3)$$

Inspection of S3 reveals that as w_0 decreases, the denominator of the right-hand side increases. This leads to a decrease in the $\bar{\theta}_d - \theta_d$. Therefore, as the w_0 decreases, θ_d increases.

With strong anchoring, the tilt angle of LC at air and a solid substrate is given by[1]

$$\theta = \frac{z}{d} 90° \qquad (S4)$$

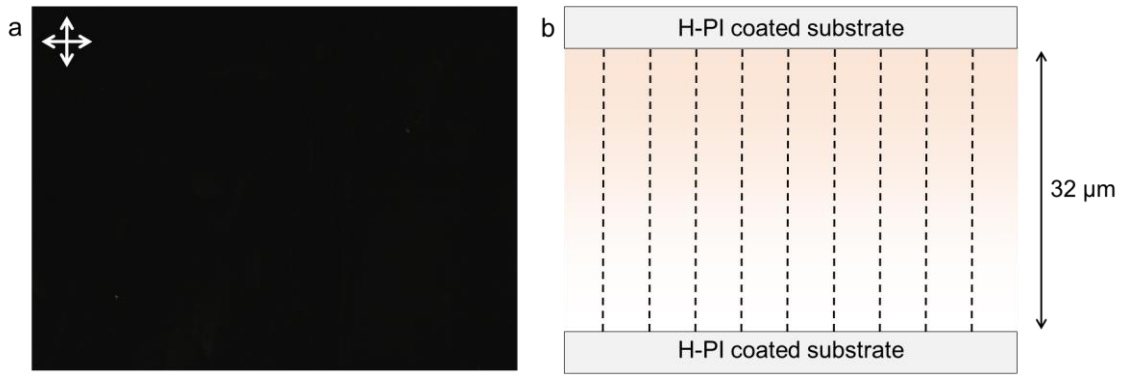

Figure S2. a) An optical micrograph (cross polars) of PCH LC sandwiched between two H-PI-coated substrates. b) A corresponding side-view schematic illustration of a).

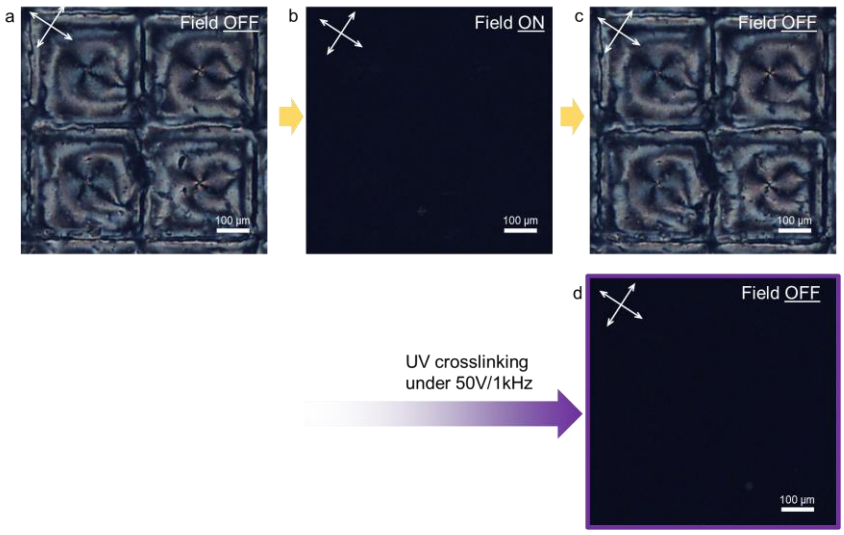

Figure S3. Optical micrographs (cross polars) of RM257/5CB sandwiched between two H-PI-coated ITO glass substrates. RM257/5CB a) before applying an electric field, b) under an electric field (50V/1kHz), c) after removing an electric field. d) RM257/5CB after crosslinking under an electric field (50V/1kHz).

The total free energy is expressed as follows,

$$U_{total} = U_{NF,elastic} + U_{LC,elastic} + U_{NF,electric} + U_{LC,electric}$$

$$= \int_0^{\theta_{f,0}} \frac{M^2}{2EA(r_0 - \hat{r}_0)} d\theta + 2\pi CK{\theta_f}^2 + \frac{V_{NF}}{2}\epsilon_0\beta_T E^2 \sin^2\theta_f$$

$$+ \frac{V_{LC}}{2}\epsilon_0\Delta\epsilon_{PCH}E^2\sin^2\theta_f \quad (S5)$$

Strain energy stored in a nanofiber: For simplification, we assumed the shape of a bent nanofiber is an arc of a circle before and after deformation by the LC. In other words, along the length of the nanofiber, the radius of curvature does not vary. At the bottom substrate, the tilt angle of the nanofiber from the surface normal is 0°. In these circumstances, the tilt angle of a bent nanofiber tip (shown in Figure S4) can be determined from the radius of curvature of the bent fiber. The bending moment is described by[2]

$$M = EA\hat{r}_0(r_0 - \hat{r}_0)\left(\frac{1}{\hat{r}} - \frac{1}{\hat{r}_0}\right) \quad (S6)$$

where E, A, r_0, $\hat{r}$, $\hat{r}_0$ are the Young's modulus (≈ 2 GPa), cross-sectional area (≈ 4 × 10^3 nm^2), a radius of curvature before deformation, a radius of curvature of neutral axis after deformation, and before deformation. The radius of curvature of a neutral axis is given by[2]

$$\hat{r} = \frac{a^2}{2(r - \sqrt{r^2 - a^2})} \quad (S7)$$

where a is the radius of a nanofiber ≈ 37 nm. The strain energy in the beam segment dθ is expressed by[2]

$$\frac{dU}{d\theta} = \frac{M^2}{2EA(r_0 - \hat{r}_0)} \quad (S8)$$

where[2]

$$U = \int_0^{\theta_{f,0}} \frac{M^2}{2EA(r_0 - \hat{r}_0)} d\theta \quad (S9)$$

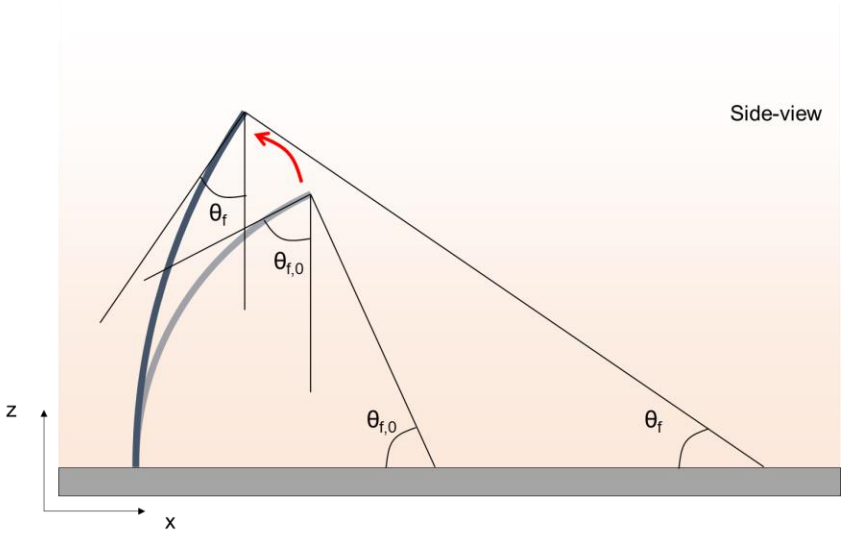

Figure S4. A schematic illustration of a bent nanofiber.

Approximation for determination of $U_{LC,elastic}$, $U_{NF,electric}$, $U_{LC,electric}$: To simplify the evaluation of $U_{LC,elastic}$, $U_{NF,electric}$, and $U_{LC,electric}$, we approximated the geometry of the bent fiber as two straight fibers with a tilt angle of θ_f (top) and 0° (bottom) as shown in Figure S5. Therefore, the effective length (L_{eff}) of a nanofiber that is strained by electric field and LC is half of the entire length (≈ L/2).

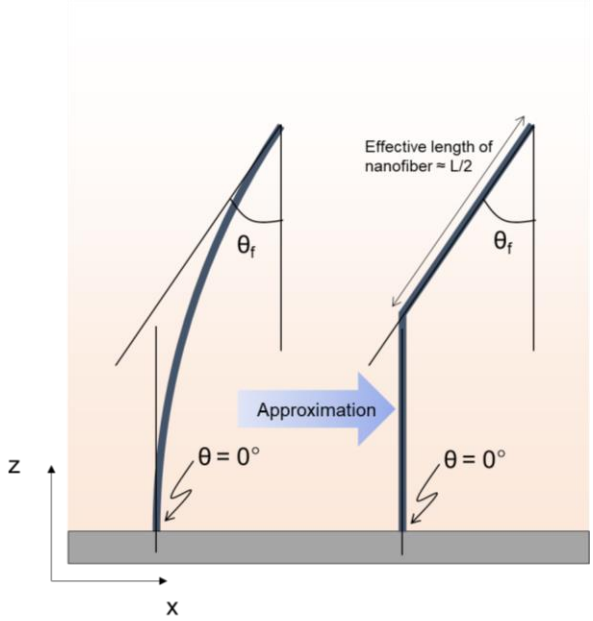

Figure S5. A schematic illustration for showing the geometrical approximation of a bent nanofiber.

Elastic energy in LC: According to Leheny and coworkers,[3] the elastic energy of LC is described by [3]

$$2\pi CK{\theta_f}^2 \quad (S10)$$

where C ≈ $L_{eff}/2\ln(L_{eff}/2a)$ is the capacitance of a NF and K is Frank elastic constant with one parameter approximation $K_{11} = K_{22} = K_{33} = K$ (≈ 10 pN).[3]

Electric energy in a nanofiber: According to Kim et al., the field-induced torque acting on an ellipsoidal inclusion is described by [4]

$$T_{NF,electric} = \frac{V}{2}\varepsilon_0\beta_T E^2 \sin 2\theta \quad (S11)$$

where ε_0, E, and V are the vacuum permittivity (≈ 8.85 × 10^{-12} F/m), electric field intensity, and volume of a single fiber ($V_{NF} = \pi a^2 \times L_{eff}$).[4] β_T is the polarizability factor for cylinders,[4]

$$\beta_T = \frac{(\varepsilon_{NF} - \varepsilon_{LC})^2}{(\varepsilon_{NF} + \varepsilon_{LC})} \quad (S12)$$

where ε_{NF} and ε_{LC} are the relative permittivities of a nanofiber (≈ 3) and relative mean permittivity of LC (≈ 12.6, $(\varepsilon_{\perp}+2\varepsilon_{\parallel})/3$). Therefore, the electrical energy is expressed by,

$$U_{NF,electric} = \int_0^{\theta_f} T_{NF,electric} d\theta = \int_0^{\theta_f} \frac{V}{2}\varepsilon_0\beta_T E^2 \sin 2\theta \, d\theta = \frac{V}{2}\varepsilon_0\beta_T E^2 \sin^2\theta_f \quad (S13)$$

Electric energy in LC near a nanofiber: The field-induced torque acting on a liquid crystal is described by,

$$T_{LC,electric} = \frac{V_{LC,eff}}{2}\varepsilon_0 \Delta\varepsilon E^2 \sin 2\theta \quad (S14)$$

where $\Delta\varepsilon=\varepsilon_{\parallel}-\varepsilon_{\perp}\approx 10.1$. We assumed that the effective volume of LC that shares the orientation of nanofiber is $V_{LC} = 8\ V_{NF} = 8\pi a^2 L_{eff}$.[5] Therefore, the electric energy is expressed by,

$$U_{LC,electric} = \int_0^{\theta_f} T_{LC,electric} d\theta = \int_0^{\theta_f} \frac{V_{LC,eff}}{2}\varepsilon_0 \Delta\varepsilon E^2 \sin 2\theta\, d\theta = \frac{V_{LC,eff}}{2}\varepsilon_0 \Delta\varepsilon E^2 \sin^2 \theta_f \quad (S15)$$

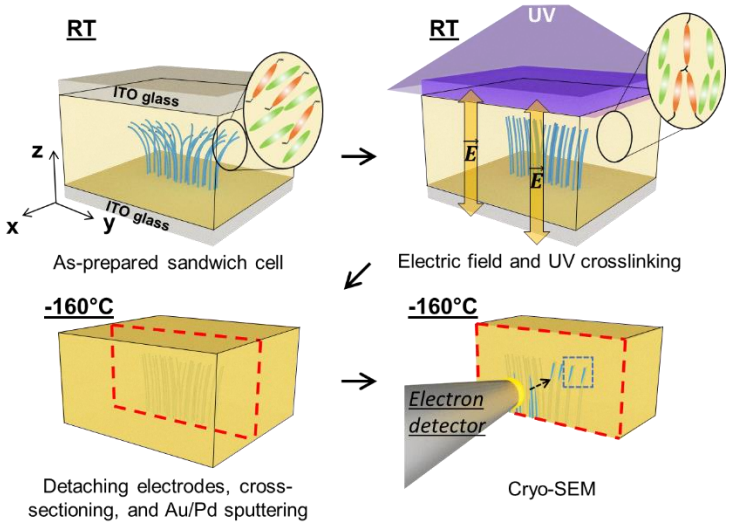

Figure S6. A schematic illustration of the sample preparation procedure for cross-sectional imaging of a cryo-SEM specimen.

Electrooptic response of PCH LC in a twisted cell: We observed the reorientation of LC on the x-y plane with an electric field applied along the z-axis when using NFF embedded in PCH (positive dielectric anisotropy). To explore whether similar phenomena also occur with standard twisted LC cells (nematic LC only), we characterized the electrooptic response of a twisted PCH film confined between two rubbed planar PI-coated substrates (thickness ≈ 100 μm) without an NFF. Here, the rubbing directions of a PI coating on each ITO glass are indicated in the schematic illustration (Figure S7). Under crossed analyzer and polarizer parallel to in-plane (x-y) orientation of LC at the top and bottom substrates, respectively, PCH phase exhibited a bright optical

appearance because of the waveguide property of the twisted LC.[6] Below the Fréedericksz transition voltage (< 2 V), the twist angle of LC was unchanged, exhibiting a bright optical appearance (Figure S7). Above the Fréedericksz transition voltage (> 2 V), the PCH exhibited a dark optical appearance under an electric field, indicating that 1) the waveguide property was lost due to the field-induced alignment and 2) the azimuthal orientation of LC on each planar PI was unchanged. Therefore, we conclude that the in-plane (x-y) orientation change perpendicular to the external electric field, observed in Figure 4a-c, is due to the presence of the nanofibers embedded in the LC.

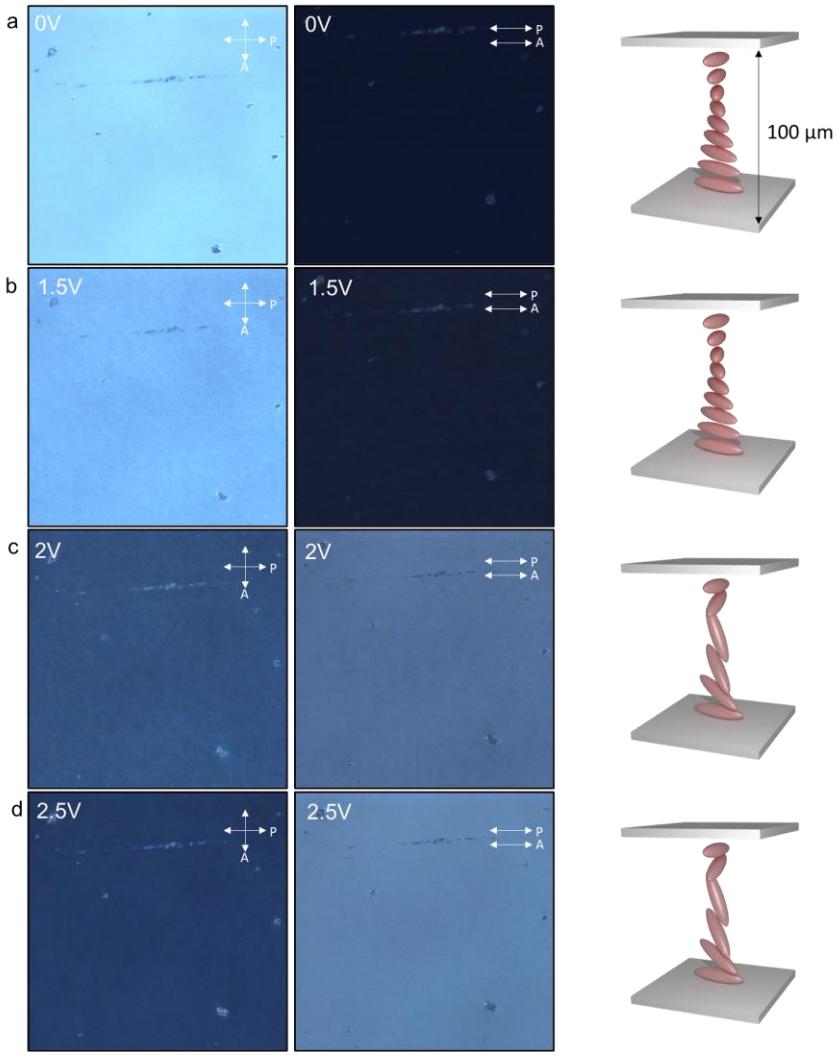

Figure S7. Electrooptic response of twisted PCH at a) 0 V, b) 1.5 V, c) 2 V, and d) 2.5 V.

Fabrication of twisted LC cell: ITO glass (15 – 25 Ω/sq, Sigma-Aldrich) was treated with planar PI (PI2555, HD MicroSystems). We rubbed the planar PI-coated substrates with a velvet cloth to encode the LC alignment. The gap between surfaces was ≈ 100 μm, which was achieved by attaching double-sided tape (3M) between the two substrates. The twist angle of the LC was determined by rotating an analyzer with a fixed polarizer angle.

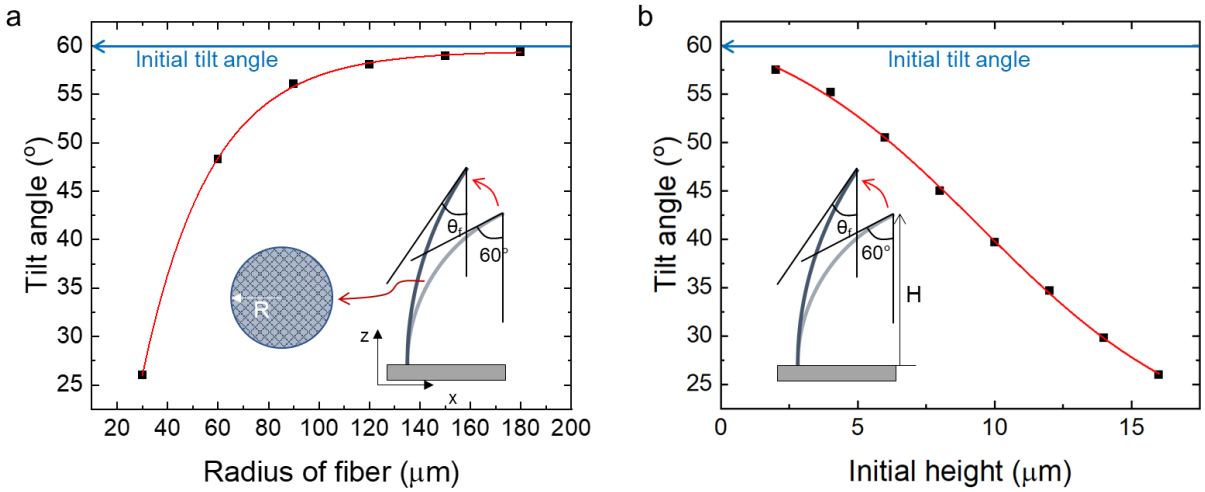

Figure S8. a) Change in tilt angle under an electric field (50 V/1kHz) vs. radius of a nanofiber. b) Change in tilt angle under an electric field (50 V/1kHz) vs. an initial height of a nanofiber. The tilt angle was estimated using equation (S5).

References

[1] M. Kleman, O. D. Lavrentovich, *Soft Matter Physics: An Introduction*, Springer, **2003**.

[2] J. R. Barber, *Intermediate Mechanics of Materials*, Springer, **2011**.

[3] C. Lapointe, A. Hultgren, D. M. Silevitch, E. J. Felton, D. H. Reich, R. L. Leheny, *Science* **2004**, *303*, 652.

[4] G. H. Kim, Y. M. Shkel, *J. Mater. Res.* **2004**, *19*, 1164.

[5] J. Y. Lee, B. Lev, J. H. Kim, *Sci. Rep.* **2019**, *9*, 20223.

[6] D. S. Miller, R. J. Carlton, P. C. Mushenheim, N. L. Abbott, *Langmuir* **2013**, *29*, 3154.